Proceedings of the Fourth Lunar Science Conference
(Supplement 4, *Geochimica et Cosmochimica Acta*)
Vol. 2, pp. 1865–1888

Ar^{39}–Ar^{40} ages and Ar^{37}–Ar^{38} exposure ages of lunar rocks

A. STETTLER, P. EBERHARDT, J. GEISS, N. GRÖGLER, and P. MAURER

Physikalisches Institut, University of Berne, Sidlerstrasse 5, 3012 Berne, Switzerland

Abstract—We have applied the Ar^{39}–Ar^{40} technique of K–Ar dating to 15 lunar rocks. The mare basalts 10071 (feldspar); 12051; 15076; and 70035 gave high temperature plateau ages of 3.51; 3.16; 3.35, and 3.74 AE respectively. Mare basalt 12018 is highly degassed and the shape of the release curve suggests a low temperature plateau at 0.65 AE. The two glass-rich basalts 12008 and 12009 show similar, complex release curves with an age minimum at intermediate temperatures. However, the total Ar^{39}–Ar^{40} age of these two rocks is in agreement with the age commonly observed for Apollo 12 basalts.

Several Apollo 14 and 15 rocks have ages compatible with the proposed 3.95 AE cataclysm. These include the Apollo 15 anorthosites 15415 and 15418. It still remains an open question whether these rocks were formed by an igneous process at this time or whether they are thoroughly outgassed remnants of the proposed original anorthositic crust of the moon.

A mare basalt-like clast from the polymict breccia 15459 collected at the Apennine Front gives an age of 3.33 AE, similar to the age of the Apollo 15 mare basalts. Thus breccia 15459 was formed a long time after the Imbrian impact.

INTRODUCTION

THE Ar^{39}–Ar^{40} METHOD of K–Ar dating (Merrihue, 1965) has become an important means of establishing lunar chronology (cf. Turner, 1970; Sutter *et al.*, 1971; Turner *et al.*, 1972; Stettler *et al.*, 1972; Huneke *et al.*, 1972; Kirsten *et al.*, 1972; Alexander *et al.*, 1972). With this method argon losses, which are the main drawback of the conventional argon-potassium dating technique, can be identified by recording the Ar^{40}/Ar^{39} temperature release curve. When a high temperature plateau is observed in such a release curve, there is generally good agreement between Ar^{39}–Ar^{40} ages and Rb–Sr ages in the case of rocks with simple histories such as the lunar mare basalts. For more complicated systems the Ar^{39}–Ar^{40} method complements Rb–Sr and U–Pb dating inasmuch as the three methods record various different steps in the history of the rock. For instance the impact which led to the formation of the Apollo 12 KREEP glass (12033) was dated by the Ar^{39}–Ar^{40} method (Eberhardt *et al.*, 1972, 1973), yielding the age of Copernicus assuming this cratering event is indeed the source of the Apollo 12 KREEP glass. Another advantage of Ar^{39}–Ar^{40} technique is its high sensitivity and it can be applied to rocks such as anorthosites which contain not enough radioactive elements for other methods (Turner, 1972; Stettler *et al.*, 1972; Husain *et al.*, 1972).

The activation with fast neutrons and the subsequent argon analysis gives not only the potassium content from the $K^{39}(n, p)Ar^{39}$ reaction but also the calcium concentration from the $Ca^{40}(n, \alpha)Ar^{37}$ reaction. The Ar^{38}/Ar^{37} ratio as well as the temperature release curve of these two isotopes can be used to derive an exposure age (Turner *et al.*, 1972). Since in most lunar rocks calcium is the dominant target element for the production of spallation argon, the Ar^{37}–Ar^{38} method has the advantage of being approximately independent of rock chemistry.

In this paper we report Ar^{39}–Ar^{40} ages and Ar^{37}–Ar^{38}_{sp} exposure ages of lunar rocks. Some of these data have been given before in an abstract (Stettler *et al.*, 1972). Our results on the Apollo 12 KREEP glass have already been reported in detail (Eberhardt *et al.*, 1973). Additional analyses of this material and the age obtained for the Apollo 17 (74220) orange soil will be published elsewhere.

EXPERIMENTAL PROCEDURE

After removal of natural rock surfaces the samples were either crushed to < 150 μm (Apollo 11, 12, and 14) or broken into a few larger pieces (Apollo 15, 16, and 17). The samples were then wrapped in aluminum foil, placed into aluminum containers under N_2 and sealed. A chain of five such containers (including two containers with hornblende standard CC 27 and one container with another hornblende standard) was placed inside the 1 millimeter cadmium shielding of a Harwell capsule and irradiated by fast neutrons in one of the isotope channels of the FR-2 reactor, Gesellschaft für Kernforschung, Karlsruhe. A Ni wire placed alongside each Al-container measured the neutron fluence (E > 0.1 MeV) at the sample position using the $Ni^{58}(n, p)Co^{58}$ reaction. For all results reported in this paper fluences were between 3×10^{18} and 1.1×10^{19} cm^{-2}. The fluence inhomogenity inside the Harwell capsule within the space occupied by the samples was ± 3.2 percent in one case and smaller than ± 1.5 percent in all the others.

Stepwise heating of the samples was carried out in a noble gas extraction system employing inductive heating. Extraction blanks for Ar^{40} in 10^{-8} cm^3 STP were the following: ≤ 0.05 (≤ 1200°C); 0.1 (at 1360°C); 0.6 (at 1600°C). The argon analysis was performed on-line with a double magnetic mass spectrometer (cf. Schwarzmüller 1970). High Ar^{40}/Ar^{39} ratios can be measured with this instrument, and thus relatively low neutron fluences can be employed. This is an advantage as it minimizes radiation damage and its possible effects on the method (cf. Alexander *et al.*, 1973). The mass spectrometer has programmable magnets and a digitized system for measuring the ion currents. All the masses from 35 to 41 were registered six to eight times and extrapolated to time zero.

In evaluating the Ar^{39}–Ar^{40} age, correction must be made for the effects of interfering fast neutron reactions (Mitchell, 1968; Brereton, 1970; Berger and York, 1970; Dalrymple and Lanphere, 1971; Turner, 1971). In order to determine the Ar isotopes produced from Ca we have irradiated several Ca-compounds and metallic Ca in the position of the reactor where our samples were activated. We obtained $(Ar^{36}/Ar^{37})_{Ca} = (2.7 \pm 0.2) \times 10^{-4}$; $(Ar^{38}/Ar^{37})_{Ca} = (6 \pm 2) \times 10^{-5}$; $(Ar^{39}/Ar^{37})_{Ca} = (6.85 \pm 0.20) \times 10^{-4}$. Other production ratios used by us are as follows: $(Ar^{40}/Ar^{37})_{Ca} \leq 5 \times 10^{-3}$ (Dalrymple and Lanphere, 1971); $(Ar^{40}/Ar^{39})_K = (6 \pm 2) \times 10^{-3}$ (Dalrymple and Lanphere, 1971; Mitchell, 1968); $(Ar^{38}/Ar^{39})_K = (1.8 \pm 0.6) \times 10^{-2}$ (from our data on terrestrial samples with high K/Ca ratios).

The $Cl^{37}(n, \gamma\beta)Ar^{38}$ reaction is only significant in lunar samples with relatively high Cl content and low exposure age. From our data on rock 61016 we obtain an upper limit of 3×10^{-12} cm^3 STP Ar^{38}/g and ppm Cl for a fluence of 10^{18} cm^{-2} under the irradiation conditions used in this work.

Decay of Ar^{37} and Ar^{39} during and after irradiation was corrected for, using $\lambda_{37} = 0.0203$ day^{-1} and $\lambda_{39} = 7.2 \times 10^{-6}$ day^{-1}. The concentrations of Ar^{39} and Ar^{37} and the $Ar^{40}*/Ar^{39}*$ and Ar^{38}_{sp}/Ar^{37} ratios were evaluated by comparison with the respective Ni activities and the hornblende monitors. For calculating Ar^{39}–Ar^{40} ages and exposure ages the following correction parameters were used: $(Ar^{36}/Ar^{38})_{sp} = 0.65 \pm 0.1$; $(Ar^{40}/Ar^{38})_{sp} = 0.2 \pm 0.1$; $(Ar^{36}/Ar^{38})_{tr} = 5.32 \pm 0.15$. The following $(Ar^{40}/Ar^{36})_{tr}$ ratios, derived from soil investigations of the respective landing sites, were used: 1^{+2}_{-1} for Apollo 11; 1 ± 0.7 for Apollo 12; 1.4 ± 0.5 for Apollo 14; 1.1 ± 0.5 for Apollo 15; 1.2 ± 0.8 for Apollo 16; 1 for Apollo 17. An "apparent Ar/K age" was calculated for each temperature step, using $\lambda = 5.305 \times 10^{-10}$ y^{-1}, $\lambda_e = 0.585 \times 10^{-10}$ y^{-1}, and $K^{40}/K = 0.0119$ mole percent.

Symbols used in this paper:
$Ar^{40}*$: Ar^{40} produced *in situ* by radioactive decay of K^{40}.
$Ar^{39}*$: Ar^{39} produced by $K^{39}(n, p)$.
Index sp: produced by spallation.
Index tr: trapped component.

Table 1. Calibration of our primary standard, the hornblende CC 27.

Reference Sample	K and Ar Isotopic Dilution Ages of Reference Sample (10^6 yr)	K/Ar Age of Hornblende Standard CC 27 (10^6 yr)	Age of Standard CC 27, Average from Irradiation Series (10^6 yr)	Sample Description and *Source*
CC 27	2650 ± 50 (2), (3)		2650 ± 50	Hornblende, *S. R. Hart*
C8C	1375 ± 40 (4)	2665		Hornblende from amphibolite, Eldora, Idaho Springs formation, *S. R. Hart*
CAA-12	1692 ± 68 (5)	2630		Biotite, Jeroma, Arizona, *M. Lanphere*
H 3089	940 ± 30 (1)	2665	2645 ± 50	Hornblende, *S. R. Hart*
P 207	81.0 ± 2.1 (6)	2635		Muscovite, interlaboratory standard, *E. Jäger*
Be 4M	17.6 ± 1.4 (7), (8), (9)	2610		Muscovite from gneiss, Brione, Valle Verzasca (Switzerland), *E. Jäger*
CAA-12	1692 ± 68	2670	2655 ± 30	cf. above
BS-1	160.2 ± 0.7 (9)	2650		Biotite from quartz diorite, Aleutian Range, Alaska, *M. Lanphere*
10003	3740 ± 60 (10)	2630		Apollo 11 Mare Basalt
10017	2350 ± 60 (11)	2690	2650 ± 80	Apollo 11 Mare Basalt
10071	2880 ± 60 (11)	2605		Apollo 11 Mare Basalt

(1) Hart, 1970.
(2) Krähenbühl, 1971.
(3) Stettler, 1973.
(4) Hart, 1964.
(5) Lanphere, 1968.
(6) Lanphere and Dalrymple, 1967.
(7) Jäger *et al.*, 1963.
(8) Signer and McDowell, 1970.
(9) Dalrymple and Lanphere, 1971.
(10) Eberhardt *et al.*, 1971.
(11) Eberhardt *et al.*, 1972a.

ABSOLUTE CALIBRATION

For the absolute calibration of the Ar^{39}–Ar^{40} method a well dated standard is required. The way in which we have calibrated our primary standard, the hornblende CC 27 is shown in Table 1. For the sake of simplicity Ar^{40*}/K^{40} data are expressed in terms of K–Ar ages using the decay constants given above. The first line gives the K–Ar age of hornblende CC 27 determined by K and Ar isotope dilution. In addition aliquots of CC 27 were irradiated in three different irradiation series together with various standard samples. Comparison of the Ar^{40*}/Ar^{39*} ratios obtained by total extraction from these standard samples with those obtained from CC 27 allowed calculation of a K–Ar age for CC 27 using the known K–Ar ages of the standards (third column in Table 1). The average for each series was derived by weighting the data obtained from the different standards with the inverse of the respective error. It is seen in Table 1 that the four independent K–Ar ages derived for hornblende CC 27 are in excellent agreement. We shall use in this paper

$$(2650 \pm 25) \times 10^6 \text{ yr}$$

for the age of this hornblende standard. The error of $\pm 25 \times 10^6$ yr is included in the errors given for the ages of the lunar samples. The error of the standard does not include uncertainties in the decay constants or isotopic abundance of K^{40}.

RESULTS

The investigated lunar samples are characterized in Table 2. The descriptions given are necessarily brief and simplified. More complete descriptions can be found in the literature referenced in the Table.

The results of the Ar^{39}–Ar^{40} investigations and the other relevant isotope data obtained by stepwise heating are given in Table 3. Each temperature step, including rise-time, lasted 1 hour. The errors were calculated by quadratically adding the 3 fold standard deviation of the measured ratio; errors due to blank, mass discrimination and non-linearity of the amplifier system; the uncertainties of interference corrections; and, in the case of the apparent age, the uncertainty of the K–Ar age of the CC 27 standard. Not included are errors due to uncertainties in the decay constants or isotopic abundance of K^{40}.

Table 4 summarizes the Ar^{39}–Ar^{40} ages, exposure ages, and Ca and K concentrations of the investigated samples. High temperature plateau ages are given if they were observed. For those samples which show a decrease in the apparent K–Ar age at high temperature an "intermediate temperature age" is given. Sometimes the distinction between these two cases is somewhat arbitrary.

Table 4 includes four duplicate analysis of rocks with high temperature plateaus. The average deviation of the duplicate age determinations is less than $\pm 0.5\%$. This shows the inherent reproducibility of our measurements. The age errors given in Table 4 are higher because they represent two to three standard deviations and they also include the age uncertainty of our CC 27 standard.

The exposure ages given in Table 4 were determined in the following way: The Ca and K concentrations in the sample were derived from Ar^{37} and Ar^{39} by comparison with the CC 27 standard, Fe and Ti concentrations were taken from

Table 2. Brief, simplified characteristics of investigated lunar samples. In column 4 data in roman type refer to the whole recovered rock, data in italics give particular characteristics of our sample. Abbreviations: MB = mare basalt, Px = pyroxene.

Number	Locality	Station	Rock Type, *Sample Characteristics*	Chemical Classification of Sample
10003,39	Tranquillity Base	LM	Group 2, type 1, ophitic basalt (2)	MB low K, high Ti
10017,43	Tranquillity Base	LM	Group 3, type 2, intersertal basalt (2)	MB high K, high Ti
10071,30	Tranquillity Base	LM	Group 3, type 3, intersertal basalt (2)	MB high K, high Ti
12008,10	N of Head Crater		Group 1, type 1, porphyritic basalt, model 65–80% glass matrix (2)	MB low K, low Ti
12009,39	N of Head Crater		Group 1, type 1, porphyritic basalt, model 65–80% glass matrix (2)	MB low K, low Ti
12018,36	N of Head Crater		Group 1, type 4, porphyritic basalt (2)	MB low K, low Ti
12051,11	SW of Surveyor Crater		Group 2, type 2, ophitic basalt (2)	MB low K, low Ti
14053,24	Flank Crater, near Cone Crater rim	C2	Coarse grained dolerite, probably clast from boulder	MB to KREEP (9)
14310,127	Smooth Terrain W of Cone Crater (6)	(G)	Fine grained, feldspatic basalt, recrystallized	KREEP
15076,10	Elbow Crater	1	Very coarse porphyritic clinopyroxene mare basalt, weakly shocked (3)	MB low K, low Ti
15382,9	Spur Crater	7	Rake sample, non-mare basalt	KREEP
15415,10	Spur Crater, NNW rim	7	"Genesis rock," anorthosite, part of breccia	Anorthitic, low K
15418,50	Spur Crater, N rim	7	Shock-melted, gabbroic anorthosite (3), part of breccia	Anorthositic, low K
15459,32	Spur Crater, NE inner wall	7	Polymict clastic breccia, *large mare basalt-like igneous clast* (1)	MB, high Px (1)
61016,4	E rim of Plum Crater	1	"Big Muley," clast-rich breccia (8), very inhomogenous	
68415,49	Cayley Plain (5), outside rim of 5 m Crater (8)	8	Anorthositic gabbro, rock chips from crystalline boulder (8)	Anorthositic
70035,6	60 m NE of LM on rim crest of 25 m Crater (7)	LM	Porphyritic subfloor basalt (4), from large boulder	MB, low K, high Ti

(1) Gast, 1972. (4) Schmitt, 1973. (7) Apollo Lunar Geology Investigation Team, 1973.
(2) Warner, 1971. (5) Elston *et al.*, 1972. (8) Apollo Lunar Geology Investigation Team, 1972.
(3) LSPET, 1972. (6) Turner *et al.*, 1971. (9) Hubbard *et al.*, 1972.

Table 3. Results from stepwise heating of neutron activated samples.

Approximate temperature (°C)	$Ar^{40}*$ (10^{-8} cm³/g)	$\frac{Ar^{40}}{Ar^{36}}$	$\frac{Ar^{38}_{sp}}{Ar^{37}}$ ($\times 10^{-2}$)	$\frac{Ar^{37}}{Ar^{39}*}$	$\frac{Ar^{40}*}{Ar^{39}*}$	Apparent Age (10^6 yr)
10071	Total rock (55.5 mg)					
400	13 ± 5	308 ± 12	—	0.40 ± 0.40	18.3 ± 8.0	570 ± 120
600	1815 ± 90	485.5 ± 8.0	8.45 ± 0.30	1.65 ± 0.080	147.3 ± 3.0	2535 ± 25
800	2410 ± 120	184.7 ± 2.5	8.70 ± 0.20	4.65 ± 0.20	257.5 ± 5.0	3365 ± 35
1000	2100 ± 110	152.8 ± 2.5	8.30 ± 0.35	11.90 ± 0.60	278.5 ± 7.0	3500 ± 45
1150	500 ± 30	32.58 ± 0.35	8.40 ± 0.35	110.3 ± 3.0	243.5 ± 12.0	3280 ± 80
1500	370 ± 30	29.4 ± 1.6	8.85 ± 0.30	178.1 ± 5.5	295 ± 20	3580 ± 90
Total	7200	123.5	8.5	18.3	216.5	3000
10071	Ilmenite concentrate CA-2 (19.0 mg)					
550	123 ± 15	435 ± 70	6.90 ± 0.40	2.10 ± 0.40	81.0 ± 8.0	2170 ± 130
650	460 ± 25	1015 ± 40	12.90 ± 0.90	0.60 ± 0.10	115.9 ± 1.2	2665 ± 30
700	615 ± 30	1160 ± 45	27.7 ± 3.5	0.300 ± 0.050	161.0 ± 3.0	3140 ± 40
750	840 ± 40	680 ± 25	8.55 ± 0.30	1.80 ± 0.10	190.2 ± 3.0	3400 ± 35
800	357 ± 20	730 ± 30	8.10 ± 0.30	2.88 ± 0.20	203.8 ± 3.0	3510 ± 35
890	452 ± 25	470 ± 20	8.07 ± 0.30	6.24 ± 0.30	201.8 ± 3.0	3495 ± 35
990	310 ± 15	94 ± 4.0	15.6 ± 0.60	15.40 ± 0.55	146.8 ± 3.0	3000 ± 40
1600	147 ± 10	12.0 ± 1.0	30.0 ± 1.2	76.7 ± 2.3	180.0 ± 8.0	3320 ± 65
Total	3300	168.5	21.1	6.2	160.0	3110
10071	Feldspar concentrate CA-4 (15.1 mg)					
600	456 ± 45	665 ± 45	20.3 ± 2.5	0.43 ± 0.07	86.0 ± 9.0	2250 ± 140
750	2320 ± 120	798 ± 30	5.90 ± 0.20	2.60 ± 0.13	143.5 ± 2.5	2975 ± 35
810	4100 ± 200	361 ± 15	5.21 ± 0.15	9.40 ± 0.50	191.5 ± 3.0	3420 ± 35
860	2920 ± 150	270 ± 10	5.00 ± 0.15	18.10 ± 0.80	209.5 ± 3.0	3560 ± 35
910	875 ± 45	278 ± 10	5.00 ± 0.20	20.20 ± 0.80	211.0 ± 3.5	3570 ± 40
1020	2420 ± 120	263 ± 10	5.15 ± 0.20	21.35 ± 0.90	201.2 ± 3.5	3495 ± 35
1600	765 ± 40	154.0 ± 8.0	5.10 ± 0.20	37.4 ± 1.1	212.0 ± 7.0	3580 ± 50
Total	13860	321.5	5.2	12.7	181.0	3330
10071	Feldspar concentrate CA-6 (9.7 mg)					
550	320 ± 35	500 ± 35	4.46 ± 0.40	1.16 ± 0.11	106.2 ± 11.0	2540 ± 150
730	6230 ± 310	648 ± 25	5.75 ± 0.30	3.50 ± 0.14	158.0 ± 3.5	3125 ± 40
790	1330 ± 65	391 ± 16	5.00 ± 0.20	9.90 ± 0.30	205.0 ± 3.0	3530 ± 35
840	1250 ± 65	304 ± 12	5.10 ± 0.20	13.30 ± 0.40	206.5 ± 3.0	3540 ± 35
900	1065 ± 55	299 ± 12	5.12 ± 0.20	15.50 ± 0.50	209.2 ± 3.5	3560 ± 40
1020	2710 ± 140	265 ± 10	5.25 ± 0.20	18.55 ± 0.55	195.0 ± 3.0	3450 ± 35
1600	850 ± 45	83.0 ± 4.0	5.28 ± 0.20	64.1 ± 1.9	200.0 ± 7.5	3490 ± 60
Total	13770	330.0	5.3	11.4	175.8	3290
12051.11	(50.7 mg)					
500	83.5 ± 5.0	298 ± 12	3.31 ± 0.16	10.05 ± 0.70	133.5 ± 8.0	2530 ± 75
730	213 ± 13	280.5 ± 6.0	3.40 ± 0.10	25.4 ± 1.5	194.0 ± 9.0	3070 ± 70
810	133.0 ± 8.0	251.0 ± 7.0	3.50 ± 0.10	34.2 ± 1.7	210.5 ± 10	3200 ± 60
870	186 ± 11	213.5 ± 4.5	3.50 ± 0.10	40.7 ± 2.0	208.5 ± 10	3180 ± 60
900	184 ± 11	218.5 ± 6.0	3.50 ± 0.10	40.8 ± 1.6	212.0 ± 8.5	3210 ± 50
980	262 ± 16	205.7 ± 3.0	3.45 ± 0.10	40.9 ± 1.4	201.5 ± 6.0	3130 ± 45

Table 3. (continued).

Approximate temperature (°C)	$Ar^{40}*$ (10^{-8} cm³/g)	$\frac{Ar^{40}}{Ar^{36}}$	$\frac{Ar^{38}_{sp}}{Ar^{37}}$ (×10^{-2})	$\frac{Ar^{37}}{Ar^{39}*}$	$\frac{Ar^{40}*}{Ar^{39}*}$	Apparent Age (10^6 yr)
1120	243±15	39.20±0.60	3.81±0.13	196.0±6.0	197.5±6.0	3100±40
1310	83.0±8.0	19.50±0.90	5.00±0.15	430±20	215.0±15.0	3230±115
Total	1390	95.5	4.04	80.3	194.7	3075
12051.11 (59.0 mg)						
550	59.0±6.0	277.0±8.0	3.82±0.30	8.70±0.80	78.5±8.0	1700±90
650	207±12	294.5±4.5	3.91±0.15	21.30±0.50	195.0±4.5	2895±35
800	333±20	249.2±3.5	3.80±0.13	34.35±0.80	231.3±3.5	3150±40
900	313±18	228.0±3.5	3.74±0.11	40.7±1.0	235.5±4.5	3180±40
1000	370±25	191.7±2.5	3.89±0.12	44.7±1.1	228±14	3130±90
1330	255±15	73.20±1.50	4.170±0.090	117.0±3.0	233±10	3160±70
Total	1535	170.0	4.05	45.6	210.7	3010
12008 (55.9 mg)						
550	54.5±9.0	710±100	0.65±0.13	23.3±4.5	174±35	4030±330
650	87.5±5.0	695±50	0.720±0.080	26.0±2.5	179±18	4080±170
700	72.5±4.5	630±50	0.555±0.045	26.3±2.5	181±18	4100±170
750	180.5±9.0	550±25	0.480±0.030	27.1±1.1	164.5±6.0	3935±60
850	244±13	660±35	0.511±0.016	27.75±0.80	114.5±2.5	3350±40
940	300±17	625±40	0.493±0.015	33.1±1.0	92.2±1.4	3020±35
1050	217±13	210±10	0.486±0.015	90.3±2.5	72.5±1.5	2665±40
1190	136.5±8.0	134.0±7.0	0.478±0.020	165.0±7.0	75.0±2.5	2715±60
1600	235±20	198±10	0.522±0.016	126.5±5.0	96.5±4.5	3090±70
Total	1530	321.5	0.496	74.0	102.3	3180
12008 (43.9 mg)						
550	66±10	675±70	0.48±0.10	25.5±5.0	185±35	3760±320
750	330±20	535±50	0.560±0.030	27.6±1.4	189±7.0	3795±60
850	243±13	537±25	0.565±0.035	29.7±1.2	145.5±4.5	3370±50
930	303±16	595±30	0.548±0.020	34.7±1.3	115.5±1.8	3015±35
1000	175±10	340±17	0.562±0.017	67.4±2.0	86.8±1.7	2600±40
1100	260±14	157.0±8.0	0.552±0.017	134.0±4.0	94.4±1.8	2720±40
1240	119.0±7.0	172.5±7.0	0.627±0.020	134.5±4.5	96.7±3.0	2755±50
1600	108±10	213.0±8.0	0.601±0.018	129.5±8.0	122.5±6.0	3105±80
Total	1600	317.5	0.572	74.0	120.8	3085
12009 (51.3 mg)						
550	64±12	116±12	2.70±0.60	23.5±4.5	165±30	3960±300
700	308±20	91.3±3.5	1.74±0.14	23.8±1.6	146.0±8.0	3765±90
800	146±10	60.1±1.2	1.625±0.050	24.9±1.0	134.7±3.5	3635±50
900	293±18	64.1±1.2	1.650±0.050	36.0±1.1	114.5±2.5	3380±40
1000	237±14	82.5±1.6	1.635±0.050	62.0±2.0	89.2±1.8	2995±40
1100	292±18	47.2±1.0	1.600±0.045	152.0±4.5	83.4±1.7	2895±40
1250	112.5±8.0	57.3±1.1	1.680±0.045	136.0±4.5	91.3±3.0	3030±50
1600	82.5±8.0	81.0±5.0	1.680±0.040	127±1.0	130±11	3570±130
Total	1540	67.0	1.63	79.4	108.3	3290

Table 3. (continued).

Approximate temperature (°C)	Ar^{40}_{*} (10^{-8} cm^3/g)	$\frac{Ar^{40}}{Ar^{36}}$	$\frac{Ar^{38}_{sp}}{Ar^{37}}$ ($\times 10^{-2}$)	$\frac{Ar^{37}}{Ar^{39}*}$	$\frac{Ar^{40}*}{Ar^{39}*}$	Apparent Age (10^6 yr)
12009 (47.5 mg)						
550	71 ± 14	340 ± 40	2.20 ± 0.45	34.0 ± 1.0	170 ± 35	3650 ± 340
700	171 ± 14	174 ± 10	1.74 ± 0.14	22.5 ± 2.0	154.0 ± 8.0	3490 ± 80
810	281 ± 17	151.5 ± 4.5	1.860 ± 0.060	25.9 ± 1.0	160.0 ± 3.5	3550 ± 45
910	234 ± 14	179.0 ± 4.5	1.840 ± 0.060	36.2 ± 1.2	141.2 ± 3.0	3350 ± 40
1000	185 ± 11	159 ± 16	1.870 ± 0.060	54.4 ± 1.8	107.3 ± 2.0	2930 ± 40
1100	425 ± 20	70.2 ± 2.0	1.810 ± 0.050	125.5 ± 4.5	105.5 ± 2.0	2905 ± 40
1240	152.0 ± 9.0	56.9 ± 1.2	1.865 ± 0.050	148.0 ± 5.0	101.0 ± 3.0	2840 ± 50
1620	51.0 ± 6.0	84.5 ± 3.5	1.860 ± 0.060	141.0 ± 9.0	140 ± 14	3330 ± 160
Total	1570	106.0	1.83	81.2	125.1	3165
12018 (49.7 mg)						
500	5.5 ± 2.5	49.5 ± 8.0	1.66 ± 0.35	7.5 ± 1.5	11.00 ± 1.60	615 ± 80
650	18.2 ± 1.6	150.0 ± 8.0	1.97 ± 0.16	7.20 ± 0.60	11.65 ± 0.45	645 ± 20
800	45.6 ± 2.5	75.5 ± 9.0	1.885 ± 0.080	20.60 ± 0.80	16.80 ± 0.40	875 ± 20
920	62.3 ± 3.5	44.4 ± 1.3	1.835 ± 0.060	38.0 ± 1.3	20.25 ± 0.45	1015 ± 25
990	74.1 ± 4.5	75.5 ± 3.5	1.820 ± 0.060	45.0 ± 1.7	41.5 ± 1.1	1695 ± 35
1100	99 ± 6.0	50.1 ± 1.0	2.030 ± 0.060	120.7 ± 4.5	82.5 ± 2.0	2565 ± 45
1600	119 ± 10	18.3 ± 1.0	2.120 ± 0.050	440 ± 30	110.0 ± 7.0	2980 ± 90
Total	420	36.0	2.02	74.7	35.5	1530
12018 (49.2 mg)						
500	5.2 ± 2.5	49.5 ± 5.0	1.80 ± 0.35	7.3 ± 1.5	10.9 ± 1.7	670 ± 90
700	49.0 ± 3.5	90.3 ± 9.0	1.73 ± 0.17	13.50 ± 0.80	13.45 ± 0.35	795 ± 25
800	24.1 ± 1.5	44.3 ± 2.5	1.71 ± 0.16	30.5 ± 1.1	15.00 ± 0.40	870 ± 25
890	63.0 ± 4.0	41.7 ± 1.2	1.785 ± 0.070	43.1 ± 1.3	20.85 ± 0.50	1125 ± 30
1000	57.0 ± 3.5	73.5 ± 2.2	1.835 ± 0.060	50.2 ± 1.7	45.7 ± 1.3	1930 ± 40
1090	58.3 ± 3.5	45.8 ± 1.0	2.000 ± 0.060	131.8 ± 4.5	81.2 ± 2.5	2695 ± 45
1250	77.0 ± 6.0	14.80 ± 0.45	2.035 ± 0.060	488 ± 30	94.0 ± 2.5	2910 ± 45
1600	52 ± 14	29.30 ± 0.90	2.095 ± 0.06	414 ± 45	164 ± 25	3770 ± 260
Total	385	33.0	1.96	77.3	32.5	1545
14053.24 (93.7 mg)						
500	200 ± 20	1215 ± 40	0.360 ± 0.040	6.20 ± 0.20	64.5 ± 6.0	2430 ± 120
650	1415 ± 65	1205 ± 16	0.197 ± 0.006	16.45 ± 0.35	162.8 ± 2.5	3830 ± 30
810	830 ± 40	1465 ± 15	0.191 ± 0.011	32.35 ± 0.70	178.7 ± 3.5	3980 ± 50
910	765 ± 35	1835 ± 30	0.198 ± 0.006	40.10 ± 0.80	178.5 ± 3.5	3980 ± 40
960	450 ± 20	2100 ± 60	0.236 ± 0.012	35.30 ± 0.70	176.0 ± 3.5	3960 ± 40
1060	445 ± 20	752.0 ± 8.0	0.252 ± 0.006	81.0 ± 1.2	166.5 ± 2.5	3870 ± 30
1150	177.0 ± 9.0	288.7 ± 2.5	0.201 ± 0.006	312.0 ± 8.0	173.0 ± 4.5	3940 ± 50
1560	127.0 ± 6.0	386 ± 12	0.196 ± 0.004	241.5 ± 5.0	156.2 ± 3.0	3770 ± 90
Total	4400	1110	0.212	47.1	159.0	3795
14053.24 (69.1 mg)						
500	58 ± 12	420 ± 60	1.90 ± 0.60	10.5 ± 2.5	165 ± 45	1800 ± 350
780	1360 ± 70	1400 ± 100	0.720 ± 0.030	27.9 ± 1.0	608 ± 20	3650 ± 60
840	710 ± 35	1235 ± 50	0.675 ± 0.050	40.3 ± 1.4	707 ± 25	3890 ± 70
910	515 ± 30	1430 ± 140	0.695 ± 0.035	44.5 ± 1.6	719 ± 25	3920 ± 70
960	605 ± 30	1800 ± 250	0.695 ± 0.030	43.6 ± 1.3	732 ± 25	3950 ± 60
1050	765 ± 40	1800 ± 130	0.760 ± 0.025	49.4 ± 1.6	735 ± 20	3950 ± 50

Table 3. (continued).

Approximate temperature (°C)	$Ar^{40}*$ (10^{-8} cm³/g)	$\frac{Ar^{40}}{Ar^{36}}$	$\frac{Ar^{38}_{sp}}{Ar^{37}}$ ($\times 10^{-2}$)	$\frac{Ar^{37}}{Ar^{39}*}$	$\frac{Ar^{40}*}{Ar^{39}*}$	Apparent Age (10^6 yr)
1170	270 ± 20	460 ± 25	0.720 ± 0.025	227 ± 14	715 ± 45	3900 ± 120
1370	275 ± 20	520 ± 25	0.700 ± 0.020	308 ± 18	740 ± 45	3960 ± 120
1570	80 ± 15	780 ± 120	0.710 ± 0.035	300 ± 30	710 ± 100	3900 ± 200
Total	4640	1130	0.72	65.3	658	3775
14310.127	(37.7 mg)					
400	190 ± 20	1545 ± 45	10.10 ± 0.90	3.10 ± 0.35	315 ± 30	2700 ± 130
650	3150 ± 310	1300 ± 130	—	8.05 ± 0.80	480 ± 50	3330 ± 170
720	3080 ± 140	1177 ± 18	7.60 ± 0.30	9.55 ± 0.30	573 ± 17	3620 ± 40
800	3550 ± 180	1038 ± 16	7.70 ± 0.30	11.40 ± 0.35	625 ± 20	3750 ± 50
890	5040 ± 250	1080 ± 12	7.90 ± 0.30	12.70 ± 0.45	672 ± 20	3880 ± 60
1010	2780 ± 140	778 ± 10	7.60 ± 0.30	11.20 ± 0.40	583 ± 12	3640 ± 40
1230	740 ± 40	193.5 ± 2.0	7.75 ± 0.30	44.3 ± 1.3	530 ± 15	3500 ± 45
1600	270 ± 15	186.0 ± 3.5	7.75 ± 0.30	58.8 ± 6.0	420 ± 40	3130 ± 160
Total	18800	760.0	6.78	12.8	578	3630
15076.10	(92.9 mg)					
650	113.0 ± 5.5	20.50 ± 0.25	2.90 ± 0.20	19.10 ± 0.90	103.3 ± 1.3	3220 ± 20
760	196 ± 10	64.80 ± 0.60	2.95 ± 0.13	25.0 ± 1.0	115.50 ± 0.70	3375 ± 35
890	366 ± 18	70.75 ± 0.60	2.820 ± 0.090	44.8 ± 1.3	116.7 ± 2.0	3400 ± 30
1000	290 ± 14	87.45 ± 0.90	2.915 ± 0.090	45.8 ± 1.4	114.3 ± 1.3	3355 ± 35
1100	175.5 ± 9.0	33.60 ± 0.30	3.18 ± 0.13	141.0 ± 5.5	112.2 ± 3.5	3345 ± 50
1260	100.0 ± 5.0	14.035 ± 0.090	3.11 ± 0.10	389 ± 12	112.4 ± 4.0	3350 ± 60
1600	104.5 ± 5.0	13.67 ± 0.15	3.07 ± 0.10	400 ± 15	110.5 ± 4.5	3325 ± 70
Total	1355	36.3	3.05	106.0	113.4	3345
15459.32	Basaltic clast (89.9 mg)					
500	19.2 ± 1.0	129.0 ± 3.5	2.905 ± 0.080	10.60 ± 0.80	48.0 ± 2.5	2130 ± 50
650	73.2 ± 3.5	121.1 ± 1.7	3.60 ± 0.22	23.9 ± 2.5	96.0 ± 8.0	3100 ± 120
750	525 ± 25	164.3 ± 1.7	3.80 ± 0.10	118.5 ± 7.0	109.6 ± 1.4	3310 ± 35
880	229 ± 10	68.90 ± 0.80	3.940 ± 0.080	115.0 ± 9.0	111.5 ± 4.0	3335 ± 60
990	50.1 ± 2.5	41.70 ± 0.35	4.10 ± 0.12	38.0 ± 4.0	105.0 ± 7.0	3240 ± 100
1090	42.1 ± 1.9	17.13 ± 0.20	4.42 ± 0.14	79.0 ± 6.0	100.5 ± 4.5	3175 ± 70
1250	21.10 ± 0.90	3.055 ± 0.070	6.71 ± 0.18	160 ± 23	85.0 ± 8.0	2920 ± 140
1600	99.0 ± 4.5	1.91 ± 0.11	4.61 ± 0.13	364 ± 22	84.5 ± 2.5	2915 ± 45
Total	1060	42.7	4.70	89.2	102.5	3200
15415.10	Anorthosite (163.0 mg)					
780	35.2 ± 2.1	12.80 ± 0.25	1.900 ± 0.060	612 ± 35	181.7 ± 7.5	2760 ± 55
870	117.0 ± 6.0	35.50 ± 0.70	1.930 ± 0.045	665 ± 20	349.8 ± 7.0	3770 ± 40
950	93.0 ± 4.5	43.20 ± 0.80	1.945 ± 0.045	642 ± 18	381.5 ± 9.5	3920 ± 50
1050	55.9 ± 3.0	42.90 ± 0.90	1.940 ± 0.050	605 ± 18	363.0 ± 7.0	3835 ± 40
1140	51.9 ± 2.5	44.3 ± 1.0	1.930 ± 0.050	615 ± 18	365.0 ± 9.0	3845 ± 50
1240	37.4 ± 2.0	41.9 ± 1.1	1.930 ± 0.050	700 ± 20	378 ± 13	3905 ± 70
1330	62.1 ± 3.0	46.6 ± 1.1	1.950 ± 0.050	635 ± 19	373.5 ± 9.0	3880 ± 50
1560	91.4 ± 5.5	50.0 ± 1.5	1.935 ± 0.045	625 ± 19	401 ± 12	4000 ± 60
Total	545	36.7	1.93	637	350	3775

Table 3. (continued).

Approximate temperature (°C)	$Ar^{40}*$ (10^{-8} cm^3/g)	$\frac{Ar^{40}}{Ar^{36}}$	$\frac{Ar^{38}_{sp}}{Ar^{37}}$ ($\times 10^{-2}$)	$\frac{Ar^{37}}{Ar^{39}*}$	$\frac{Ar^{40}*}{Ar^{39}*}$	Apparent Age (10^6 yr)
15415.10	Anorthosite (105.3 mg)					
800	24.5 ± 2.5	18.30 ± 0.60	1.635 ± 0.050	551 ± 15	121.5 ± 4.5	2400 ± 50
880	84.0 ± 4.5	36.80 ± 0.90	1.690 ± 0.040	655 ± 20	271 ± 10	3595 ± 65
960	111.5 ± 5.5	45.1 ± 1.4	1.700 ± 0.045	637 ± 20	321 ± 10	3870 ± 70
1060	62.0 ± 3.5	46.80 ± 0.90	1.705 ± 0.045	660 ± 20	346 ± 12	3995 ± 70
1130	68.0 ± 4.0	46.65 ± 0.90	1.705 ± 0.040	657 ± 20	343 ± 12	3980 ± 70
1230	42.0 ± 4.0	40.6 ± 1.9	1.740 ± 0.050	736 ± 30	340 ± 25	3960 ± 140
1340	55.0 ± 5.5	44.9 ± 1.7	1.740 ± 0.050	671 ± 25	341 ± 20	3970 ± 120
1600	90 ± 18	47.0 ± 4.5	1.61 ± 0.16	650 ± 65	350 ± 35	4010 ± 200
Total	545	40.1	1.710	646	337	3950
15418.50	(192.1 mg)					
500	2.10 ± 0.30	57.3 ± 3.0	2.10 ± 0.25	48.5 ± 5.5	36.0 ± 4.0	1780 ± 100
950	8.10 ± 0.40	12.82 ± 0.20	2.035 ± 0.060	220 ± 12	38.8 ± 2.0	1870 ± 50
1080	9.90 ± 0.40	6.67 ± 0.10	2.090 ± 0.040	1130 ± 45	103.0 ± 4.0	3215 ± 65
1200	49.5 ± 2.5	6.17 ± 0.12	2.120 ± 0.040	1360 ± 40	137.7 ± 4.5	3675 ± 55
1270	49.3 ± 2.5	11.50 ± 0.35	2.095 ± 0.040	1075 ± 25	171.8 ± 4.0	4035 ± 50
1340	60.3 ± 3.0	11.97 ± 0.25	2.085 ± 0.040	1050 ± 30	173.0 ± 5.0	4050 ± 55
1440	58.7 ± 2.5	12.62 ± 0.30	2.070 ± 0.050	945 ± 20	163.0 ± 4.0	3950 ± 45
1600	9.10 ± 0.60	14.75 ± 0.25	2.040 ± 0.070	720 ± 110	144 ± 25	3750 ± 300
Total	246.0	9.85	2.090	958	115.1	3385
15382.9	Crystalline KREEP fragment (7.43 mg)					
550	445 ± 25	960 ± 80	6.15 ± 1.20	1.05 ± 0.20	50.0 ± 1.8	2085 ± 40
650	1120 ± 50	1055 ± 60	5.20 ± 0.25	1.12 ± 0.35	86.0 ± 1.7	2825 ± 30
760	4020 ± 180	646 ± 12	2.67 ± 0.20	3.320 ± 0.070	139.4 ± 1.6	3565 ± 35
870	1675 ± 80	531 ± 15	2.39 ± 0.19	9.03 ± 0.16	166.0 ± 3.0	3850 ± 35
970	1845 ± 100	468 ± 11	2.245 ± 0.060	17.70 ± 0.40	171.0 ± 4.0	3895 ± 50
1230	1225 ± 60	224.0 ± 8.0	2.210 ± 0.070	33.9 ± 1.0	166.0 ± 4.5	3850 ± 50
1340	2145 ± 110	915 ± 30	2.200 ± 0.070	9.13 ± 0.25	143.3 ± 3.5	3610 ± 45
1570	25.0 ± 5.0	600 ± 120	6.5 ± 2.9	0.83 ± 0.20	50 ± 12	2080 ± 240
Total	12500	550	2.41	8.23	133.0	3505
61016.4	(94.2 mg)					
500	10.2 ± 1.3	45.9 ± 2.5	7.6 ± 1.5	3.40 ± 0.45	35.5 ± 4.5	1600 ± 110
650	29.8 ± 1.8	63.2 ± 2.5	2.57 ± 0.11	3.03 ± 0.12	42.20 ± 0.80	1800 ± 20
810	274 ± 14	181.5 ± 3.5	0.900 ± 0.012	3.760 ± 0.040	92.45 ± 0.70	2840 ± 30
900	334 ± 18	447.0 ± 8.0	0.460 ± 0.070	10.560 ± 0.040	138.8 ± 1.1	3460 ± 40
1050	137.0 ± 7.0	29.60 ± 0.40	0.101 ± 0.010	117.7 ± 1.5	130.5 ± 2.5	3360 ± 40
1160	192.0 ± 9.0	450 ± 16	0.066 ± 0.002	141.8 ± 1.7	148.5 ± 1.9	3570 ± 40
1300	755 ± 45	5800 ± 350	0.026 ± 0.001	198.0 ± 2.0	156.5 ± 2.0	3650 ± 40
1600	41.0 ± 3.5	5500 ± 1000	0.007 ± 0.001	460 ± 11	157 ± 11	3660 ± 140
Total	1775	216.2	0.060	103.0	128.5	3340
68415.49	(162.6 mg)					
650	109.5 ± 5.0	576.5 ± 4.5	0.900 ± 0.020	39.20 ± 0.35	165.8 ± 1.5	2970 ± 30
800	603 ± 30	308.6 ± 1.6	1.260 ± 0.009	90.30 ± 0.60	252.4 ± 1.7	3630 ± 40
900	440 ± 25	137.8 ± 1.1	1.365 ± 0.015	218.3 ± 1.5	281.8 ± 1.7	3800 ± 40
1120	138.0 ± 7.0	78.75 ± 0.50	1.418 ± 0.013	231.8 ± 3.0	246.0 ± 2.5	3580 ± 40

Table 3. (continued).

Approximate temperature (°C)	$Ar^{40}*$ (10^{-8} cm³/g)	$\frac{Ar^{40}}{Ar^{36}}$	$\frac{Ar^{38}_{sp}}{Ar^{37}}$ ($\times 10^{-2}$)	$\frac{Ar^{37}}{Ar^{39}*}$	$\frac{Ar^{40}*}{Ar^{39}*}$	Apparent Age (10^6 yr)
1310	275 ± 15	95.40 ± 0.80	1.440 ± 0.010	281.5 ± 2.0	271.0 ± 2.0	3740 ± 40
1600	51.5 ± 3.0	88.0 ± 2.5	1.423 ± 0.014	315.5 ± 7.0	266.5 ± 8.0	3710 ± 70
Total	1620	153.0	1.362	164.9	251.9	3620
70035.6 (116.1 mg)						
500	30.5 ± 3.0	125 ± 14	5.1 ± 3.0	3.45 ± 0.70	97 ± 10	1600 ± 110
670	6.5 ± 5.0	590 ± 50	3.6 ± 1.1	2.89 ± 0.12	161.0 ± 5.0	2205 ± 45
770	251 ± 18	1220 ± 60	2.64 ± 0.11	8.62 ± 0.25	348.0 ± 7.0	3315 ± 50
850	370 ± 25	1140 ± 45	2.50 ± 0.10	20.55 ± 0.60	443.5 ± 8.0	3705 ± 50
960	277 ± 20	650 ± 25	2.45 ± 0.10	39.3 ± 1.2	468.5 ± 8.0	3790 ± 45
1060	239 ± 17	362 ± 14	2.615 ± 0.080	62.7 ± 1.9	446 ± 15	3710 ± 60
1250	159 ± 11	37.3 ± 1.5	3.095 ± 0.080	564 ± 17	428 ± 11	3645 ± 50
1600	136 ± 10	64.0 ± 3.0	3.220 ± 0.080	337 ± 12	447 ± 14	3715 ± 60
Total	1530	182.0	3.02	96.5	374	3430
70035.6 (216.8 mg)						
500	14.0 ± 2.0	210 ± 42	1.95 ± 0.25	5.70 ± 0.90	91.5 ± 9.0	1540 ± 110
670	43.8 ± 3.0	830 ± 40	2.30 ± 0.25	7.85 ± 0.30	181.5 ± 8.0	2370 ± 50
780	266 ± 19	724 ± 30	2.425 ± 0.070	30.5 ± 1.0	403.5 ± 8.0	3550 ± 45
870	206 ± 15	432 ± 17	2.415 ± 0.060	65.5 ± 2.0	472 ± 10	3810 ± 45
950	152 ± 11	332 ± 13	2.415 ± 0.060	84.5 ± 2.5	471.5 ± 8.0	3805 ± 40
1060	152 ± 11	271 ± 10	2.555 ± 0.080	95.3 ± 3.5	451 ± 12	3730 ± 50
1250	87.5 ± 6.0	41.0 ± 1.6	3.070 ± 0.070	533 ± 16	438.5 ± 9.0	3685 ± 45
1600	158 ± 11	42.4 ± 1.7	3.110 ± 0.080	523 ± 18	444.0 ± 8.0	3705 ± 40
Total	1080	137.5	2.92	149	399	3535

Symbols used:
Ar^{40}: Ar^{40} in sample, corrected for Ar^{40} produced in reactor.
$Ar^{40}*$: Ar^{40} produced by *in situ* radioactive decay of K^{40}
$Ar^{39}*$: Ar^{39} produced by $K^{39}(n, p)$
Ar^{38}_{sp}: Ar^{38} in sample produced by spallation.
Ar^{37}: Ar^{37} produced in reactor
Ar^{36}: Ar^{36} in sample, corrected for Ar^{36} produced in reactor.

the literature, and then the exposure age was calculated from (cf. Eberhardt *et al.*, 1972a)

$$T_e = \frac{Ar^{38}_{sp}}{P_{Ca}(Ca+K) + P_{Ti}Ti + P_{Fe}Fe}$$

using

$$\left.\begin{array}{l} P_{Ca} = 1.4 \\ P_{Ti} = 0.16 \\ P_{Fe} = 0.06 \end{array}\right\} \frac{10^{-8}\ \text{cm}^3\ \text{STP}\ Ar^{38}_{sp}}{\text{g (Element)}\ 10^6\ \text{y}}$$

The exposure age can also be calculated from the Ar^{38}_{sp}/Ar^{37} release curve (Turner *et al.*, 1972). In this case one sample with known exposure age (e.g., Kr^{81}

Table 4. Ar^{39}–Ar^{40} ages, exposure ages, and calcium and potassium concentrations of lunar rocks. It should be noted that Ca and K concentrations refer to the investigated samples and may not be exactly representative for the rock as a whole.

Sample		Age, High Temp. Plateau (10^9 yr)	Intermediate Temp. Age (10^9 yr)	Ar^{38}_{sp} Exposure Age (10^6 yr)	Ca (%)	K ppm
10071.30	Total	(3.47±0.11)	—	425	7.5	2300
10071.30	CA 2 Ilm.	—	(3.50±0.07)	340	1.2	1020
10071.30	CA 4 Plag.	3.53±0.06	—	360	9.1	3800
10071.30	CA 6 Plag.	3.49±0.08	—	380	8.1	3720
12051.11	*	3.16±0.05	—	205	7.3	450
12051.11	*	3.15±0.07	—	205	7.3	480
12008.10	*	—	3.18±0.07†	50	7.4	520
12008.10	*	—	3.09±0.07†	50	6.9	470
12009.39	*	—	3.29±0.07†	160	7.5	480
12009.39	*	—	3.17±0.07†	140	8.4	530
12018.36	*	—	—	170	6.6	450
12018.36	*	—	—	180	6.3	410
14053.24	*	3.93±0.06	—	25	8.0	900
14053.24	*	3.94±0.04	—	23	8.3	920
14310.127		—	3.88±0.06	250	8.5	4000
15415.10	*	(3.99±0.06)	—	100	14.1	115
15415.10	*	(3.91±0.10)	—	100	14.0	115
15418.50		(3.99±0.07)	4.04±0.06	250	11.1	55
15382.9		—	3.90±0.05	230	5.1	3200
15076.10		3.35±0.04	—	330	7.6	365
15459.32		—	3.33±0.06	520	5.5	315
61016.4		(3.65±0.04)	—	≤ 7	10.6	580
68415.49		(3.70±0.10)	3.80±0.04	90	11.5	370
70035.6	*	3.72±0.07	—	100	7.4	390
70035.6	*	3.75±0.07	—	95	7.6	260

*Independent determinations.

†Total Ar^{39}–Ar^{40} ages.

Values in parentheses: Corresponding plateau not very well defined, see Table 3 and appropriate Figure.

age) must be analysed for absolute calibration. Good agreement was found between the exposure ages calculated by the two methods.

An exposure age calculated from Ar^{38} can be affected by the production of Ar^{38} from Cl^{37} in the pile irradiation. With their low chlorine contents and relatively high exposure ages this effect is negligible in most lunar rocks under the irradiation conditions used in this work. However, in rock 61016 a large fraction of the Ar^{38} observed after irradiation is probably due to pile-neutron capture by Cl^{37},

because this rock has a low exposure age ($T_e \leq 7 \times 10^6$ y) and a high chlorine content (320 ppm, Jovanovic and Reed, 1973).

There is in fact evidence for neutron produced Ar^{38} in the argon isotope observations: (1) The strong decrease of the Ar^{38}_{sp}/Ar^{37} ratio in the release curve (Fig. 1) has not been observed for any other rock. Since a large portion of the chlorine in rock 61016 is leachable (Jovanovic and Reed, 1973), it is plausible that neutron produced Ar^{38} is earlier released than Ar^{38} produced by spallation of Ca, Ti, and Fe. (2) In the temperature step at 1300°C argon is released with an uncorrected Ar^{36}/Ar^{38} ratio of 0.39. Such a low ratio does not result from spallation, i.e., an excess of Ar^{38} produced by pile-neutrons is indicated. We intend to measure the $Cl^{37}(n, \gamma\beta)Ar^{38}$ production rate under our irradiation conditions by introducing high-chlorine standards.

Discussion

Comparison with other age determinations

In Table 5 we compare our Ar^{39}–Ar^{40} results with Ar^{39}–Ar^{40} ages and Rb–Sr ages of the same rocks published by other authors. The agreement among the Ar^{39}–Ar^{40} ages is very good, perhaps with the following exceptions: Our two high temperature plateau ages of rock 12051 (Fig. 2) obtained from two different irradiation series are lower than the age reported by Turner (1971) and Alexander *et al.* (1972). In the case of rock 14310 our temperature release curve (Fig. 3) is in quantitative agreement with those of other authors, except Husain *et al.* (1972), who find a somewhat lower age.

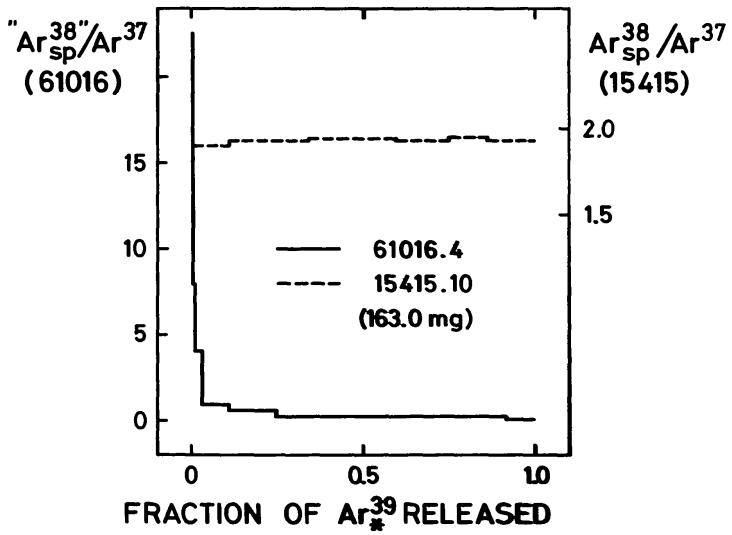

Fig. 1. Ar^{38}_{sp}/Ar^{37} release curves of two lunar rock samples. For the anorthosite 15415 the Ar^{38}/Ar^{37} ratio is constant in the whole temperature range, because in this rock virtually all the Ar^{38}_{sp} is produced from calcium, as is Ar^{37}. Rock 61016 has a high chlorine content and a low exposure age. Thus, Ar^{38} produced by pile-neutrons from Cl^{37} cannot be neglected for this rock, and the contribution of neutron produced Ar^{38} to "Ar^{38}_{sp}" is probably responsible for the unusual release curve.

Table 5. Comparison of Ar^{39}–Ar^{40} ages obtained in this work with Ar^{39}–Ar^{40} ages and internal isochron Rb–Sr ages of the same rocks published by other authors.

Sample	Ar^{39}–Ar^{40} Age High or Intermediate Temp. This work (10^9 yr)	Ar^{39}–Ar^{40} Age High or Intermediate Temp. (10^9 yr)	Rb–Sr–Age (10^9 yr)
10071	(3.47±0.11)		3.68±0.02 (11)
	Plag. 3.51±0.06		
12051	3.16±0.05	3.27±0.05 (1)	3.26±0.10 (11)
		3.29±0.06 (2)	3.58±0.30 (12)
14053	3.94±0.04	3.94±0.05 (3)	3.96±0.04 (13)
		Plag. 3.95±0.05 (3)	
		3.92±0.08 (4)	
14310	3.88±0.06	3.89±0.04 (3)	3.87±0.04 (13)
		3.78±0.03 (4)	3.93±0.04 (14)
		3.91±0.05 (5)	3.93±0.06 (15)
		Plag. 3.87±0.05 (6)	3.84±0.04 (16)
15415	(3.95±0.07)	4.09±0.19 (4)	
		4.05±0.15 (7)	
15382	3.90±0.05	3.89±0.04 (8)	
15076	3.35±0.04	3.35±0.15 (9)	3.33±0.08 (20)
68415	3.80±0.04	3.83±0.10 (9)	3.84±0.01 (17)
		3.82±0.04 (10)	
70035	3.74±0.07		3.81±0.20 (18)
			3.83±0.10 (19)
			3.82±0.06 (21)

(1) Turner, 1971.
(2) Alexander *et al.*, 1972.
(3) Turner *et al.*, 1971.
(4) Husain *et al.*, 1972.
(5) York *et al.*, 1972.
(6) Turner *et al.*, 1972.
(7) Turner, 1972.
(8) Turner *et al.*, 1973.
(9) Kirsten *et al.*, 1973.
(10) Huneke *et al.*, 1973.
(11) Papanastassiou and Wasserburg, 1971.
(12) Compston *et al.*, 1971.
(13) Papanastassiou and Wasserburg, 1971a.
(14) Compston *et al.*, 1972.
(15) Murthy *et al.*, 1972.
(16) Tatsumoto *et al.*, 1972.
(17) Papanastassiou and Wasserburg, 1972.
(18) Nyquist *et al.*, 1973.
(19) Chappel *et al.*, 1973.
(20) Papanastassiou and Wasserburg, 1972a.
(21) Murthy *et al.*, 1973.

It has been established for some time (Turner, 1970; Papanastassiou and Wasserburg, 1971) that there is good agreement between internal isochron Rb–Sr ages and Ar^{39}–Ar^{40} ages, if the latter are deriveed from a well developed high temperature plateau. This observation is remarkable in two ways: (1) Uncertainties in the decay constants of Rb^{87} and K^{40} are not even included in the errors given for the ages. (2) The internal isochron Rb–Sr age defines the time at which the investigated rock minerals separated from an isotopically mixed reservoir and became a closed system with respect to Rb and Sr. The Ar^{39}–Ar^{40} high temperature plateau age determines the time of the last complete loss of Ar from the investigated ma-

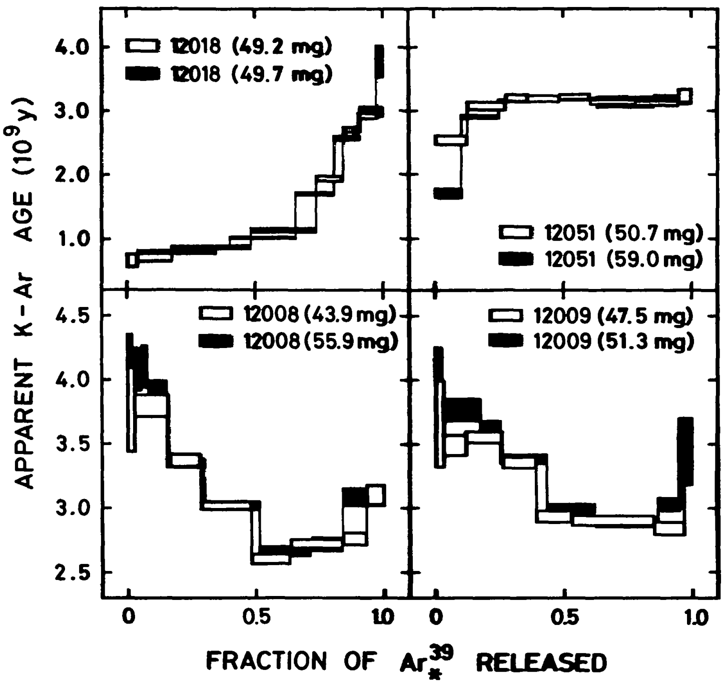

Fig. 2. Ar^{39}–Ar^{40} release curve of four basaltic rocks from the Apollo 12 landing site. The two independently determined release patterns are in good agreement in all cases. The release curve obtained for 12051 is typical for crystalline mare rocks. 12018 shows an Ar^{40} loss higher than hitherto observed for mare basalts. 12008 and 12009 give unusual release curves. These two rocks are very similar in structure, they contain 65 to 80 percent glass.

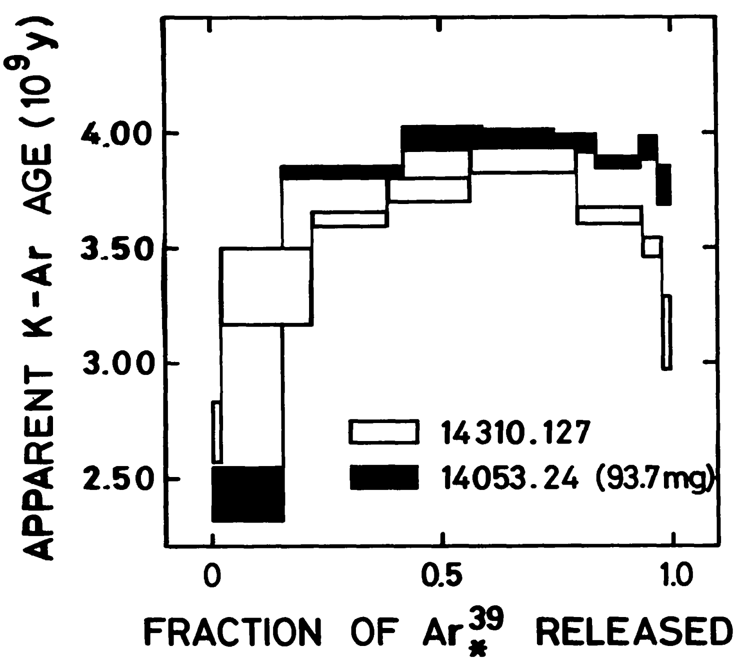

Fig. 3. Ar^{39}–Ar^{40} release curves of two Fra Mauro rocks. 14310 is recrystallized and its apparent K–Ar age shows the decrease at high temperature typical for such rocks. The chemical composition of 14053 is between those of mare basalts and KREEP, unusual for rocks of its location and age.

terial. In spite of this difference in definition the two ages usually agree very well for crystalline mare basalts, in accordance with the indicated simple history of these rocks. This concordance of the Rb–Sr and Ar^{39}–Ar^{40} ages underlines the basic validity of the ages derived from the two methods. As shown in Table 5, our Ar^{39}–Ar^{40} results agree within the limits of error with Rb–Sr ages published for the same rocks, except for the mare basalt 10071 where even in the separated feldspars we find an age younger than that obtained by Papanastassiou and Wasserburg (1971) with the Rb–Sr method.

Ages of separated minerals

Turner *et al.* (1972) were the first to investigate the Ar^{39}–Ar^{40} release curves of minerals separated from lunar rocks. They found that plagioclases give high temperature plateaus even in those rocks which show a maximum $Ar^{40}*/Ar^{39}*$ ratio at intermediate temperatures. In these cases the "intermediate temperature age" of the whole rock agrees approximately with the plagioclase high temperature age. It is for this reason that we may use in our discussion not only the high temperature plateau ages, but also the intermediate temperature maxima of the release curves. Recently, Huneke *et al.* (1973) found an exception to the rule of feldspars giving flat high temperature plateaus. For feldspar separated from rock 68415 they found a plateau at 4.09 AE with a steep rise to 4.51 AE at the highest temperature. It cannot yet be decided whether this observation is due to some redistribution mechanism or whether the high age value represents the original age of a strongly outgassed rock or rock component. For the whole rock 68415 we obtained an Ar^{39}–Ar^{40} release curve (Fig. 4) which is virtually identical with the one given by Huneke *et al.* (1973).

We have investigated the Ar^{39}–Ar^{40} release curves of a whole rock sample and separated minerals of mare basalt 10071 (Fig. 5). The mineral separates were aliquots of samples investigated by Eberhardt *et al.* (1972a), who describe separation procedures and purity of these separates. While the whole rock gives only a poorly developed plateau, the feldspar samples CA-4 ($2.46 \leqslant \rho \leqslant 2.91$; $>90\%$ feldspar) and CA-6 ($2.91 \leqslant \rho \leqslant 2.99$; $>80\%$ feldspar) give good high temperature plateaus at 3.53 ± 0.06 AE and 3.49 ± 0.08 AE respectively. The drop at high temperature in the apparent K–Ar age of the ilmenite separate can be clearly recognized in the release curve of the whole rock, indicating that ilmenite associated components contribute to the large fluctuations in the release curve of the whole rock at high temperatures (cf. Turner *et al.*, 1972).

Mare basalts

Our results on the mare rocks 10071, 12051, and 15076 essentially confirm the ages of basalt formation at the Apollo 11, 12, and 15 landing sites measured by other investigators (Wasserburg and Papanastassiou, 1971; Papanastassiou and Wasserburg, 1971a; Turner, 1970, 1971; Turner *et al.*, 1972). Our result on 10071 agrees with the observation of Turner (1971) that at the Apollo 11 landing site the

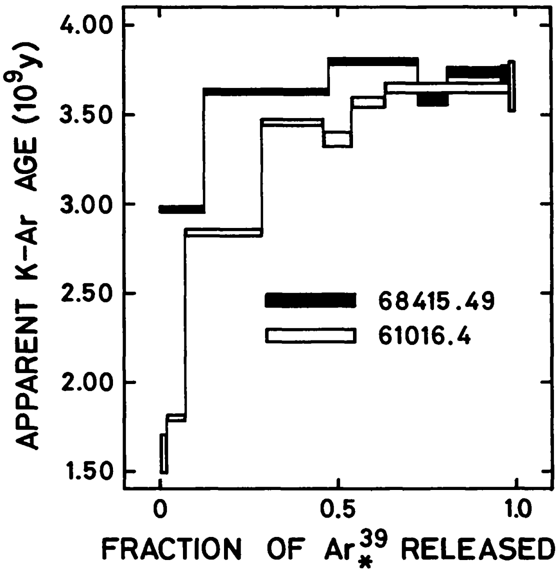

Fig. 4. Apparent Ar^{39}–Ar^{40} age of two Apollo 16 rocks.

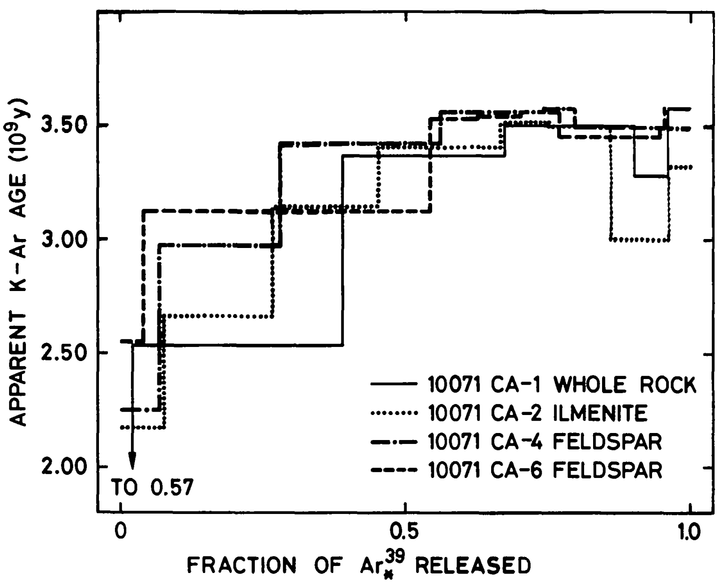

Fig. 5. Argon release curves of different components of the 10071 basalt. The limits of error can be found in Table 3. The two feldspar-rich fractions give a better high temperature plateau than the unseparated rock.

high-potassium basalts tend to give lower Ar^{39}–Ar^{40} ages than the low-potassium basalts.

It is interesting to note that the age of rock 70035, a low-K, high-Ti subfloor basalt (Fig. 6), is similar to the ages of the low-K, high-Ti basalts found at Tranquillity Base.

The basaltic rocks 12018, 12008 and 12009 give very irregular Ar^{39}–Ar^{40} release curves (Fig. 2) of a type hitherto not observed for mare basalts. Duplicate determinations made on all three rocks confirmed these complex release curves (cf. Fig. 2). The shape of the release curve of rock 12018 suggests a low temperature

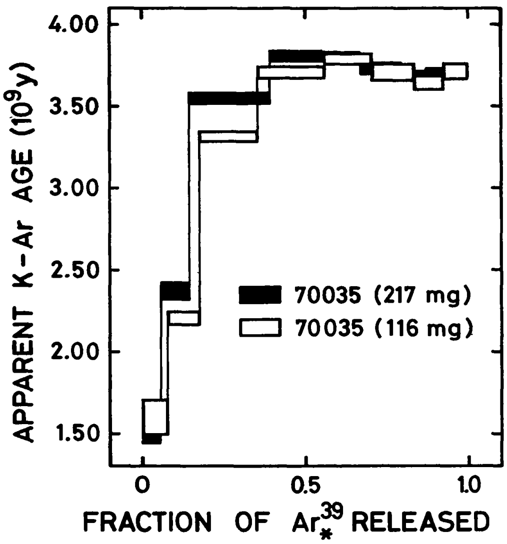

Fig. 6. Ar^{40}–Ar^{39} release curves of two samples of the 70035 subfloor basalt. The age is similar to those of basalts found at Tranquillity Base.

plateau with an age of 0.65 AE (ordinate intercept). Only at the highest temperature does the age reach that of common Apollo 12 basalts (~ 3.2 AE). This rock must have sustained rather severe gas loss as recently as 0.65 AE ago. The gas loss could have been induced by moderate heating over long time periods (e.g., deep burial, volcanism) or by shock. The exposure age of rock 12018 is close to 0.2 AE (cf. Table 3 and Lugmair and Marti, 1971) and thus smaller than the above mentioned low temperature age. However, rock 12018 was exposed to a moderately high neutron flux on the moon (Lugmair and Marti, 1971) and must have received at least a fraction of its exposure to cosmic rays in a partially shielded location. The isotopic and age data are compatible with a model history, where the rock was initially formed together with the other Apollo 12 basalts, excavated 0.65 AE ago from a deeper layer, exposed to the cosmic radiation until approximately 0.1 AE ago in a fairly shielded location, and then brought to the surface.

The release curves of the basalts 12008 and 12009 are very similar in their irregularity (cf. Fig. 2). This is consistent with the observation that these two rocks have a similar and uniquely high glass content (cf. Table 2). The glass is thought to be primary in origin (Brett *et al.*, 1972), i.e., it was formed at the time of the cooling of these rocks from a lava. Rb–Sr investigations of these rocks did not yield internal isochrons (Papanastassiou and Wasserburg, 1971).

The $Ar^{40}*/Ar^{39}*$ ratios found for rocks 12008 and 12009 at low temperatures (cf. Fig. 2) are higher than the consolidation age of the rocks, assuming that they were formed at about the same time as the other Apollo 12 basalts. It is interesting to note that the total $Ar^{40}*/Ar^{39}*$ ratios of 12008 and 12009 give ages of 3.1 AE and 3.3 AE, very close to the ages of normal Apollo 12 rocks. The overall shape of the Ar^{39}–Ar^{40} release curves of these two mare basalts is very similar to those observed for both the matrix and the chondrules of the unequilibrated chondrite Chainpur (Podosek, 1971). As in the two lunar rocks 12008 and 12009 the total K–Ar age of Chainpur is in fair agreement with its expected formation age of 4.6

AE (Heymann and Mazor, 1968; Zähringer, 1968; Podosek, 1971). A distinctly negative slope for the major part of the Ar^{39}–Ar^{40} release curve was also observed for two fragments from breccia 14321 and an Apollo 14 soil fragment (Turner *et al.*, 1971). These three Apollo 14 samples have total Ar^{39}–Ar^{40} ages compatible with the probable age of Apollo 14 rocks. Perhaps the mechanism leading to the irregular shape of the argon release curves are similar in all these samples.

The 3.95 AE cataclysm

It has been noticed before that there exists in different rock types from various locations on the lunar surface a strong grouping of Rb–Sr and Ar^{39}–Ar^{40} ages around 3.95 AE, indicating that one or several events (including the Imbrian impact) occurring at that time have obliterated much of the preceeding history of the lunar surface (cf. Tera *et al.*, 1973). There is remarkable agreement on these data between Rb–Sr and Ar^{39}–Ar^{40} ages in spite of the fact that most of the rocks giving this age are breccia with an apparently complicated history.

Our results include several rocks giving either a high temperature plateau age or an intermediate temperature peak near 3.95 AE (cf. Table 4, Figs. 3, 7, 8, and 9). Of particular interest among these are the anorthosite samples 15415 and 15418. The alkali content in these rocks is so small (cf. Table 4) that Rb–Sr ages have not been measured. The only age information comes from the Ar^{39}–Ar^{40} release curves and from common-lead model age measurements on rock 15415 (Tera *et al.*, 1972; Tatsumoto *et al.*, 1972a). In Fig. 10 the $Ar^{37}/Ar^{39}*$ ratio, expressed in terms of the corresponding Ca/K ratio, is plotted as a function of the fractional release of $Ar^{39}*$. The curve for 15076 is rather typical for mare basalts and shows that K is located on sites having lower gas retentivity than the Ca sites. The Ca/K ratio of the anorthosite 15415 (and similarly of 15418) is remarkably constant. This indicates that the potassium in this rock does not reside in some accessory mineral or interstitial material, but is incorporated in the anorthite. Thus, the Ar^{39}–Ar^{40} results of these anorthosites are directly related to the history of the dominant mineral species in this rock. The question is whether (a) these anorthosites were formed by an igneous process 4.0 billion years ago or whether (b) we deal with old material from an original lunar anorthositic crust (Wood *et al.*, 1971), which was thoroughly outgassed and/or recrystallized 4.0 billion years ago. Rock 15418 is reported to have been shock-melted (Ahrens *et al.*, 1973), an observation which increases the plausibility of hypothesis (b). Also the slight slope of the high temperature plateau observed by Turner (1972) and by ourselves (Fig. 8) for rock 15415 could be considered as an indication of a higher primary age. Ar^{39}–Ar^{40} ages higher than 4 AE have actually been reported by Husain *et al.* (1973) for 2–4 mm lithic fragments collected at the Apollo 16 landing site. On the other hand, the common lead model ages obtained by Tera *et al.* (1972) and Tatsumoto *et al.* (1972a) do not support a primary formation of this anorthosite as early as 4.6 AE ago.

Thus, it is as yet hard to decide between hypotheses (a) and (b). Actually from the data available so far, it is difficult to conclude whether the episode 3.95 AE ago consisted mainly of impact induced metamorphism on a grand scale, or whether

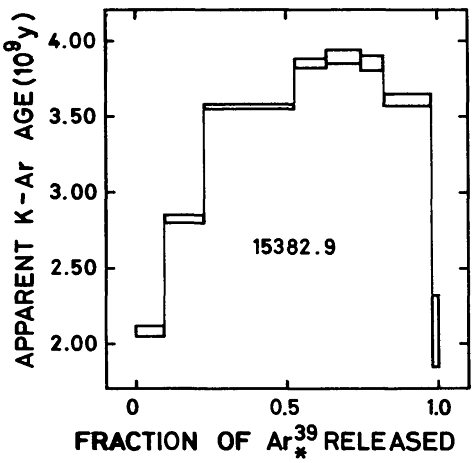

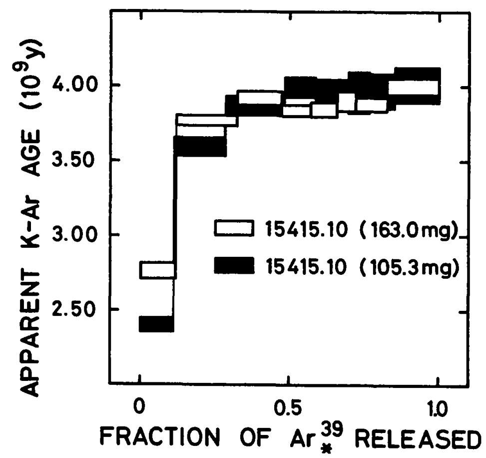

Fig. 7. Apparent age curve of 15382, a basalt with KREEP chemistry from the Apennine Front.

Fig. 8. Ar^{39}–Ar^{40} release curves of two samples of the "Genesis Rock", an anorthosite from the Apennine Front. The indicated increase at high temperatures is discussed in the text.

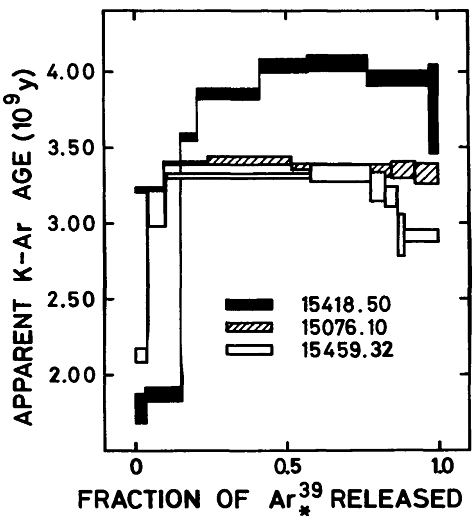

Fig. 9. Argon release curves of a mare basalt from the rim of Hadley Rille (15076) and an anorthositic clast (15418) and a mare basalt-like clast (15459) from breccias found at the Apennine Front. The ages of the mare basalt-like clast and of the basalt found in the plains are similar, i.e., breccia 15459 must have formed much later than the time of the Imbrian impact.

also significant indigeneous geochemical differentiation and igneous rock formation took place during this relatively short interval.

The data obtained from rock 14053 may help in answering this question. Among the rocks with Ar^{39}–Ar^{40} or Rb–Sr ages of about 3.95 AE, so far 14053 is the only one with a chemical composition resembling that of mare basalts. According to Bence and Papike (1972) this rock crystallized at a relatively shallowed depth. Schürmann and Hafner (1972) postulated that it was reheated, probably by the Imbrian event, transported to the Fra Mauro region and quenched. Its locality

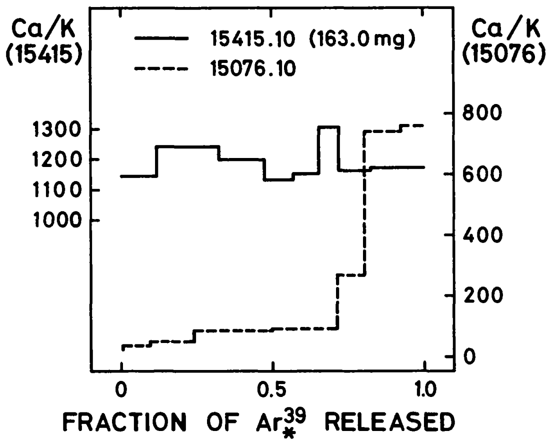

Fig. 10. Ar^{37}/Ar^{39*} release curves expressed in terms of Ca/K ratios. Mare basalt 15076 shows a pattern similar to those of other mare basalts. The anorthosite 15415 gives a constant Ca/K ratio, indicating that K is not located in accessory minerals but in the anorthite.

on the lunar surface (Table 2) suggests, that it was brought to the surface by the Cone Crater impact. The age information on this rock would agree with this historical sequence. The Ar^{39}–Ar^{40} and Rb–Sr ages are close to 3.95 AE, and the exposure age of 24 million years (cf. Table 4) and the place of recovery are indeed sufficient proof for a local, Cone Crater origin. Chemical composition and ages of rock 14053 imply that differentiation has created lava masses of chemical composition similar to mare basalts early in the lunar history, i.e., before the Imbrian impact took place.

A young clast from the Apennine Front

Sample 15459,32 is a mare basalt-like clast (Gast, 1972) in a polymict clastic breccia found at the Apennine front (cf. Table 2). The chemical composition of this clast does in fact resemble that of basalts found near the rim of Hadley Rille (Hubbard and Gast, 1972). In Fig. 9 the Ar^{39}–Ar^{40} release curves of this sample are compared with those of the rim basalt 15076 and the anorthositic clast 15418. The figure demonstrates that the intermediate temperature plateau of the clast 15459 corresponds closely to the age of Palus Putredinis basalts, and falls far below the age of approximately 3.95 AE found in all the other rocks from the Apennine front investigated so far. Thus, breccia 15459 must have been formed a long time after the Imbrian impact took place.

Acknowledgments—We should like to thank the National Aeronautics and Space Administration for generously supplying the lunar samples for this investigation. Terrestrial standards were kindly provided by Stanley R. Hart, Emilie Jäger, and Marvin A. Lanphere. We are indebted to Paul W. Gast for some special samples, and we thank him, Norman J. Hubbard, and Lawrence E. Nyquist for discussions. Luc Weber has provided the software for the computerized mass spectrometer output. We are grateful to Eveline Giger, Helene Spycher, H. Hofstetter, E. Lenggenhager, A. Schaller, U. Schwab, and M. Zuber for their help in various aspects of this work.

This research was supported by the Swiss National Science Foundation (Grants NF 2.405.70, 2.592.71, and 2.768.72).

REFERENCES

Ahrens T. J., O'Keefe J. D., and Gibbons R. V. (1973) Shock compression of a recrystallized breccia from Apollo 15 (abstract). In *Lunar Science—IV*, p. 18. The Lunar Science Institute, Houston.

Alexander E. C. Jr., Davis P. K., and Reynolds J. H. (1972) Rare-gas analyses on neutron irradiated Apollo 12 samples. *Proc. Third Lunar Sci. Conf., Geochim. Cosmochim. Acta*, Suppl. 3, Vol. 2, pp. 1787–1795. MIT Press.

Alexander E. C. Jr., Davis P. K., Reynolds J. H., and Srinivasan B. (1973) Radiogenic xenon and argon in 14318 and implications (abstract). In *Lunar Science—IV*, p. 30. The Lunar Science Institute, Houston.

Apollo Lunar Geology Investigation Team (1972) U.S. Geological Survey, *Interagency report: Astrogeology* **51**.

Apollo Lunar Geology Investigation Team (1973) U.S. Geological Survey, *Interagency report: Astrogeology* **71**.

Bence A. E. and Papike J. J. (1972) Pyroxenes as recorders of lunar basalt petrogenesis: Chemical trends due to crystal-liquid interaction. *Proc. Third Lunar Sci. Conf., Geochim. Cosmochim. Acta*, Suppl. 3, Vol. 1, pp. 431–469. MIT Press.

Berger G. W. and York D. (1970) Precision of the $^{40}Ar/^{39}Ar$ dating technique. *Earth Planet. Sci. Lett.* **9**, 39–44.

Brereton N. R. (1970) Corrections for interfering isotopes in the $^{40}Ar/^{39}Ar$ dating method. *Earth Planet. Sci. Lett.* **8**, 427–433.

Brett R., Butler P. Jr., Meyer Ch. Jr., Reid A. M., Takeda H., and Williams R. J. (1972) Apollo 12 igneous rocks 12004, 12008, 12009, and 12022: A mineralogical and petrological study. *Proc. Second Lunar Sci. Conf., Geochim. Cosmochim. Acta*, Suppl. 2, Vol. 1, pp. 301–317. MIT Press.

Chappel B. W., Compston W., Green D. H., Rudowski R., Vernon M. J., and Ware N. (1973) *Proc. Fourth Lunar Sci. Conf., Geochim. Cosmochim. Acta.* In press.

Compston W., Berry H., and Vernon M. J. (1971) Rubidium–strontium chronology and chemistry of lunar material from the Ocean of Storms. *Proc. Second Lunar Sci. Conf., Geochim. Cosmochim. Acta*, Suppl. 2, Vol. 2, pp. 1471–1485. MIT Press.

Compston W., Vernon M. J., Berry H., Rudowski R., Gray C. M., and Ware N. (1972) Apollo 14 mineral ages and the thermal history of the Fra Mauro formation. *Proc. Third Lunar Sci. Conf., Geochim. Cosmochim. Acta*, Suppl. 3, Vol. 2, pp. 1487–1501. MIT Press.

Dalrymple G. B. and Lanphere M. A. (1971) $^{40}Ar/^{39}Ar$ technique of K–Ar dating: A comparison with the conventional technique. *Earth Planet. Sci. Lett.* **12**, 300–308.

Eberhardt P., Geiss J., Grögler N., Krähenbühl U., Mörgeli M., and Stettler A. (1971) Potassium–argon age of Apollo 11 rock 10003. *Earth Planet. Sci. Lett.* **11**, 245–247.

Eberhardt P., Eugster O., Geiss J., Grögler N., Schwarzmüller J., Stettler A., and Weber L. (1972) When was the Apollo 12 KREEP ejected? In *Lunar Science—III*, pp. 206–208. The Lunar Science Institute, Houston.

Eberhardt P., Geiss J., Graf H., Grögler N., Krähenbühl U., Schwaller H., and Stettler A. (1972a) Noble gas investigations of lunar rocks 10017 and 10071. Submitted to *Geochim. Cosmochim. Acta.*

Eberhardt P., Geiss J., Grögler N., and Stettler A. (1973) How old is the crater Copernicus? Submitted to *The Moon.*

Elston D. P., Bondette E. L., and Schafer J. P. (1972) Geology of the Apollo 16 Landing Site Area, U.S. Geol. Survey, Open-File Rept.

Gast S. R. (1972) Private communication.

Hart S. R. (1964) The petrology and isotopic-mineral age relations of a contact zone in the front range, Colorado. *J. of Geology* **72**, 493–525.

Hart S. R. (1970) Private communication.

Heymann D. and Mazor E. (1968) Noble gases in unequilibrated ordinary chondrites. *Geochim. Cosmochim. Acta* **32**, 1–19.

Hubbard N. J. and Gast P. W. (1972) Non-mare basalts: Part II. *Proc. Third Lunar Sci. Conf., Geochim. Cosmochim. Acta*, Suppl. 3, Vol. 2, pp. 1161–1179. MIT Press.

Huneke J. C., Podosek F. A., and Wasserburg G. J. (1972) Gas retention and cosmic-ray exposure ages of a basalt fragment from Mare Fecunditatis. *Earth Planet. Sci. Lett.* **13**, 375–383.

Huneke J. C., Podosek F. A., and Wasserburg G. J. (1973) An argon bouillabaisse including ages from the Luna 20 site (abstract). In *Lunar Science—IV*, p. 403. The Lunar Science Institute, Houston.

Husain L., Schaeffer O. A., Funkhouser J., and Sutter J. (1972) The ages of lunar material from Fra Mauro, Hadley Rille, and Spur Crater. *Proc. Third Lunar Sci. Conf., Geochim. Cosmochim. Acta*, Suppl. 3, Vol. 2, pp. 1557–1567. MIT Press.

Husain L. and Schaeffer O. A. (1973) ^{40}Ar–^{39}Ar crystallization ages and ^{38}Ar–^{37}Ar cosmic ray exposure ages of samples from the vicinity of the Apollo 16 landing site (abstract). In *Lunar Science—IV*, p. 406. The Lunar Science Institute, Houston.

Jäger E., Niggli E., and Baethge H. (1963) Two standard minerals, biotite and muscovite, for Rb–Sr and K–Ar age determinations, sample Bern 4B and Bern 4M from a gneiss from Brione, Valle Verzasca (Switzerland). *Schweiz. Min. Petr. Mitt.* **43**, 465–470.

Jovanovic S. and Reed G. W. Jr. (1973) Trace element studies in Apollo 16 samples (abstract). In *Lunar Science—IV*, p. 418. The Lunar Science Institute, Houston.

Kirsten T., Deubner J., Horn P., Kaneoka I., Kiko J., Schaeffer O. A., and Thio S. K. (1972) The rare gas record of Apollo 14 and 15 samples. *Proc. Third Lunar Sci. Conf., Geochim. Cosmochim. Acta*, Suppl. 3, Vol. 2, pp. 1865–1889. MIT Press.

Kirsten T., Horn P. and Kiko J. (1973) Ar^{40}–Ar^{39} dating of Apollo 16 and Apollo 15 rocks and rare gas analysis of Apollo 16 soils (abstract). In *Lunar Science—IV*, p. 438. The Lunar Science Institute, Houston.

Krähenbühl U. (1971) Private communication.

Lanphere M. A. and Dalrymple G. B. (1967) K–Ar and Rb–Sr measurements on P-207, the U.S.G.S. interlaboratory standard muscovite. *Geochim. Cosmochim. Acta* **31**, 1091–1094.

Lanphere M. A. (1968) Geochronology of the Yavapai Series of central Arizona. *Canadian J. Earth Sci.* **5**, 757–762.

Lugmair G. W. and Marti K. (1971) Neutron capture effects in lunar gadolinium and the irradiation histories of some lunar rocks. *Earth Planet. Sci. Lett.* **13**, 32–42.

LSPET (Lunar Sample Preliminary Examination Team) (1972) Preliminary examination of lunar samples from Apollo 16. *Apollo 16 Preliminary Science Report*, NASA SP-315.

Merrihue C. M. (1965) Trace-element determinations and potassium–argon dating by mass spectroscopy of neutron-irradiated samples (abstract). *Trans. Am. Geophys. Union* **46**, 125.

Mitchell J. G. (1968) The argon-40/argon-39 method for potassium–argon age determination. *Geochim. Cosmochim. Acta* **32**, 781.

Murthy V. R., Evensen N. M., Bor-Ming J., and Coscio M. R. Jr. (1972) Apollo 14 and 15 samples: Rb–Sr ages, trace elements, and lunar evolution. *Proc. Third Lunar Sci. Conf., Geochim. Cosmochim. Acta*, Suppl. 3, Vol. 2, pp. 1503–1514. MIT Press.

Murthy V. R., Evensen N. M., and Coscio M. R. Jr. (1973) Data presented at Fourth Lunar Sci. Conf.

Nyquist L. E., Hubbard N. J., and Gast P. W. (1973) Data presented at Fourth Lunar Sci. Conf.

Papanastassiou D. A. and Wasserburg G. J. (1971) Lunar chronology and evolution from Rb–Sr studies of Apollo 11 and 12 samples. *Earth Planet. Sci. Lett.* **11**, 37–62.

Papanastassiou D. A. and Wasserburg G. J. (1971a) Rb–Sr ages of igneous rocks from the Apollo 14 mission and the age of the Fra Mauro formation. *Earth Planet. Sci. Lett.* **12**, 36–48.

Papanastassiou D. A. and Wasserburg G. J. (1972) The Rb–Sr age of a crystalline rock from Apollo 16. *Earth Planet. Sci. Lett.* **16**, 289–298.

Papanastassiou D. A. and Wasserburg G. J. (1972a) Rb–Sr age and initial strontium in basalts from Apollo 15. *Earth Planet. Sci. Lett.* **17**, 324–337.

Podosek F. A. (1971) Neutron-activation potassium–argon dating of meteorites. *Geochim. Cosmochim. Acta* **35**, 157–173.

Schmitt H. S. (1973) Presented at Fourth Lunar Sci. Conf.

Schürmann K. and Hafner S. S. (1972) Distinct subsolidus cooling histories of Apollo 14 basalts. *Proc. Third Lunar Sci. Conf., Geochim. Cosmochim. Acta*, Suppl. 3, Vol. 1, pp. 493–506. MIT Press.

Schwarzmüller J. (1970) Ein Edelgasanalysensystem mit automatischer Datenerfassung und Edelgasmessungen an Strukturelementen des Apollo-11-Mondstaubes. Ph.D. Thesis, University of Berne.

Signer P. and McDowell F. W. (1970) On-line extraction system for rapid high-precision routine analysis. *Eclogae Geol. Helv.* **63**/1, 311–321.

Stettler A., Eberhardt P., Geiss J., and Grögler N. (1972) Ar^{39}/Ar^{40} ages of Apollo 11, 12, 14, and 15 rocks (abstract). In *Lunar Science—III*, p. 724. The Lunar Science Institute, Houston.

Stettler A. (1973) Ar^{40}/Ar^{39}-Altersbestimmungen an Mondproben. Ph.D. Thesis, University of Berne.

Sutter J. F., Husain L., and Schaeffer O. A. (1971) $^{40}Ar/^{39}Ar$ ages from Fra Mauro. *Earth Planet. Sci. Lett.* **11**, 249–253.

Tatsumoto M., Hedge C. E., Doe B. R., and Unruh D. M. (1972) U–Th–Pb and Rb–Sr measurements on some Apollo 14 lunar samples. *Proc. Third Lunar Sci. Conf., Geochim. Cosmochim. Acta*, Suppl. 3, Vol. 2, pp. 1531–1555. MIT Press.

Tatsumoto M., Hedge C. E., Knight R. J., Unruh D. M., and Doe B. R. (1972a) U–Th–Pb, Rb–Sr, and K measurements on some Apollo 15 and Apollo 16 samples. In *The Apollo 15 Lunar Samples*, p. 391. The Lunar Science Institute, Houston.

Tera F., Ray A. L., and Wasserburg G. J. (1972) Distribution of P–U–Th in lunar anorthosite 15415 and interferences about its age. In *The Apollo 15 Lunar Samples*, p. 396. The Lunar Science Institute, Houston.

Tera F., Papanastassiou D. A., and Wasserburg G. J. (1973) A lunar cataclysm at ~ 3.95 AE and the structure of the lunar crust (abstract). In *Lunar Science—IV*, p. 723. The Lunar Science Institute, Houston.

Turner G. (1970) Argon-40/argon-39 dating of lunar rock samples. *Proc. Apollo 11 Lunar Sci. Conf., Geochim. Cosmochim. Acta*, Suppl. 1, Vol. 2, pp. 1665–1684. Pergamon.

Turner G. (1971) ^{40}Ar–^{39}Ar ages from the Lunar Maria. *Earth Planet. Sci. Lett.* **11**, 169–191.

Turner G., Huneke J. C., Podosek F. A., and Wasserburg G. J. (1971) ^{40}Ar–^{39}Ar ages and cosmic ray exposure ages of Apollo 14 samples. *Earth Planet. Sci. Lett.* **12**, 19–35.

Turner G. (1972) ^{40}Ar–^{39}Ar age and cosmic ray irradiation history of the Apollo 15 anorthosite, 15415. *Earth Planet. Sci. Lett.* **14**, 169–175.

Turner G., Huneke J. C., Podosek F. A., and Wasserburg G. J. (1972) Ar^{40}–Ar^{39} systematics in rocks and separated minerals from Apollo 14. *Proc. Third Lunar Sci. Conf., Geochim. Cosmochim. Acta*, Suppl. 3, Vol. 2, pp. 1589–1612. MIT Press.

Turner G., Cadogan P. H., and Yonge C. J. (1973) Argon selenochronology. Preprint.

Warner J. L. (1971) Lunar cristalline rocks: Petrology and geology. *Proc. Second Lunar Sci. Conf., Geochim. Cosmochim. Acta*, Suppl. 2, Vol. 1, pp. 469–480. MIT Press.

Wasserburg G. J. and Papanastassiou D. A. (1971) Age of an Apollo 15 mare basalt; lunar crust and mantle evolution. *Earth Planet. Sci. Lett.* **13**, 97–104.

Wood J. A., Dickey J. S. Jr., Marvin U. B., and Powell B. N. (1971) Lunar anorthosites and a geophysical model of the moon. *Proc. Apollo 11 Lunar Sci. Conf., Geochim. Cosmochim. Acta*, Suppl. 1, Vol. 1, pp. 965–988. Pergamon.

York D., Kenyon W. J., and Doyle R. J. (1972) ^{40}Ar–^{39}Ar ages of Apollo 14 and 15 samples. *Proc. Third Lunar Sci. Conf., Geochim. Cosmochim. Acta*, Suppl. 3, Vol. 2, pp. 1613–1622. MIT Press.

Zähringer J. (1968) Rare gases in stony meteorites. *Geochim. Cosmochim. Acta* **32**, 209–237.